Mechanism of Dioxirane Oxidation of CH Bonds: Application to Homo- and Heterosubstituted Alkanes as a Model of the Oxidation of Peptides

Gennady V. Shustov and Arvi Rauk*

Department of Chemistry, The University of Calgary, Alberta T2N 1N4, Canada

Received February 18, 1998

Ab initio methods have been employed to study the oxidation of the CH bonds in homo- (**1a**−**d**) and heterosubstituted alkanes (**2a**−**d, 3a,b**) by the parent dioxirane as a model for the dioxirane oxidation of proteins. The study involved methane (**1a**), ethane (**1b**), propane (**1c**), isobutane (**1d**), methylamine (**2a**), methanol (**2b**), ethanol (**2c**), acetaldehyde (**2d**), glycolaldehyde (**3a**), and a peptide model, *N*-formylglycine amide (**3b**). Geometries were optimized at DFT (B3LYP) and MP2 levels of theory using 6-31G* and 6-311+G** basis sets. Stationary points were characterized by vibrational frequency analysis. Final energies for the oxidation of **1a** were obtained at the MP4-(SDTQ)/6-311+G** and QCISD(T)/6-311+G** levels. A new mechanism of the oxidation reconciling the apparently contradictory experimental data was found. The reaction proceeds via a highly polar asynchronous transition state, which is common for either concerted oxygen insertion into the CH bond and formation of a radical pair (alkyl radical + α-hydroxyalkoxyl radical). These channels appear at a bifurcation point on the potential energy surface after the common transition state, which corresponds to formation of the new O−H bond, and ruptures of the C−H bond in the substrate and of the O−O bond in the dioxirane. The B3LYP theoretical model gives substantial hydride transfer character to the transition state and describes adequately the selectivity of the oxidation of hydrocarbons, alcohols, 1,2-diols, and leucine derivatives. The agreement with experimental data is further improved by taking into account the influence of a dielectric medium (IPCM model). The electrophilicity of dioxiranes in the oxidations of CH bonds implies that side groups of protected amino acids and proteins are more probable points for the attack of these oxidants than the weak α-CH bonds. It is of interest that selectivities of dioxirane oxidation are incorrectly predicted by the MP2 method, which overestimates the proton-transfer character of the transition state.

Introduction

Dioxiranes have been widely employed as effective regio- and stereoselective oxidants of aliphatic CH bonds.[1] The possibility that dioxiranes may be used in the synthesis of unnatural amino acids and peptides via hydroxylation of natural compounds is spurred by a recent report[2] on the oxyfunctionalization of leucine derivatives by 3,3-dimethyldioxirane. The high regioselectivity for the γ-CH bond to the total exclusion of attack on the weaker α-CH bond caught our attention. An understanding of the mechanism and of the factors that influence the selectivity of the reaction is important if dioxiranes were to be applied to such syntheses.

Dioxirane oxidations are typically carried out with an excess of the dioxirane (typically 3,3-dimethyldioxirane (DMD) or 3-(trifluoromethyl)-3-methyldioxirane (TFMD)) near room temperature in a solvent of moderate polarity, such as CH_2Cl_2 or acetone (1,1,1-trifluoroacetone). High yields of the target oxidation products[1] and stereospecificity[3] of the reaction (i.e., complete retention of configuration of the chiral center upon oxidation of an optically active hydrocarbon[3c]) allowed us to assume a concerted oxygen insertion (Scheme 1a) via an "oxenoid" transition state.[3] The available evidence for this mechanism has been summarized in papers of Curci et al.[4a] and Asensio et al.[4b]

However, observation of the formation of bromoalkanes when alkanes were reacted with DMD in the presence of CCl_3Br[5a,c] and an influence of molecular oxygen and radical inhibitors on the efficacy of the dioxirane oxidation[5b,c] led to a conclusion about a free-radical ("oxygen rebound") mechanism (Scheme 1b). This mech-

* To whom correspondence should be addressed.Tel: (403) 220-6247. Fax: (403) 289-9488. E-mail: rauk@chem.ucalgary.ca

(1) (a) Murray, R. W. *Chem. Rev.* **1989**, *89*, 1187. (b) Adam, W.; Curci, R.; Edwards, J. O. *Acc. Chem. Res.* **1989**, *22*, 205. (c) Curci, R. In *Advances in Oxygenated Processes*; Baumstark, A. L., Ed.; JAI: Greenwich, CT, 1990; Vol. 2, Chapter 1. (d) Adam, W.; Hadjiarapoglou, L. P.; Curci, R.; Mello, R. In *Organic Peroxides*; Ando, W., Ed.; Wiley: New York, 1992; pp 195−219. (e) Curci, R.; Dinoi, A.; Rubino, M. F. *Pure Appl. Chem.* **1995**, *67*, 811.

(2) Mezzetti, M.; Mincione, E.; Saladino, R. *J. Chem. Soc., Chem. Commun.* **1997**, 1063.

(3) (a) Mello, R.; Fiorentino, M.: Fusco, C.; Curci, R. *J. Am. Chem. Soc.* **1989**, *111*, 6749. (b) Mello, R.; Cassidei, L.; Fiorentino, M.; Fusco, C.; Hummer, W.; Jäger, V.; Curci, R. *J. Am. Chem. Soc.* **1991**, *113*, 2205. (c) Adam, W.; Asensio, G.; Curci, R.; González-Núñez, M. E.; Mello, R. *J. Org. Chem.* **1992**, *57*, 953. (d) Murray, R. W.; Gu, D. *J. Chem. Soc., Perkin Trans. 2* **1994**, 451.

(4) (a) Curci, R.; Dinoi, A.; Fusco, C.; Lillo, M. A. *Tetrahedron Lett.* **1996**, *37*, 249. (b) Asensio, G.; Mello, R.; González-Núñez, M. E.; Boix, C.; Royo, J. *Tetrahedron Lett.* **1997**, *38*, 2373. (c) Murray, R. W.; Jeyaraman, R.; Mohan, L. *J. Am. Chem. Soc.* **1986**, *108*, 2470 (d) Mello, R.; Cassidei, L.; Fiorentino, M.; Fusco, C.; Curci, R. *Tetrahedron Lett.* **1990**, *31*, 3067.

(5) (a) Minisci, F.; Zhao, L.; Fontana, F.; Bravo, A. *Tetrahedron Lett.* **1995**, *36*, 1697. (b) Bravo, A.; Fontana, F.; Fronza, G.; Mele, A.; Minisci, F. *J. Chem. Soc., Chem. Commun.* **1995**, 1573. (c) Bravo, A.; Fontana, F.; Fronza, G.; Minisci, F.; Zhao, L. *J. Org. Chem.* **1998**, *63*, 254. (d) Vanni, R.; Garden, S. J.; Banks, J. T.; Ingold, K. U. *Tetrahedron Lett.* **1995**, *36*, 7999.

S0022-3263(98)00287-4 CCC: $15.00
Published on Web 07/17/1998

Scheme 1

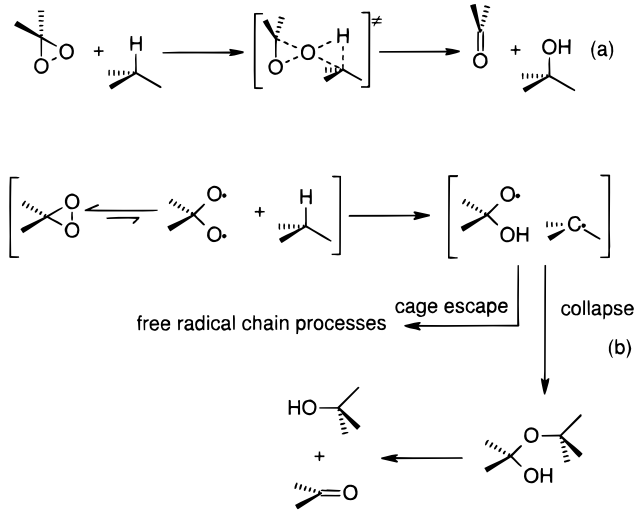

Scheme 2

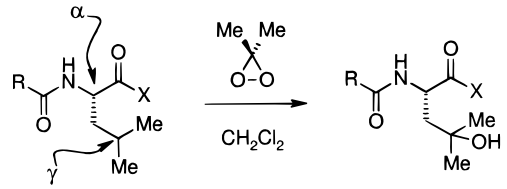

anism involves molecule-induced homolysis of the O−O bond in the dioxirane and formation and recombination of the radical pair within a solvent cage.[5]

Numerous kinetic data[3d,4] are consistent with both mechanisms. However, the γ-regiospecificity[2] of the oxidation of the leucine derivatives by DMD (Scheme 2) can be considered as an argument in favor of the concerted mechanism. Indeed, according to our theoretical estimates[6] of bond dissociation energies for the α- and γ-CH bonds in *N*-formylleucine amide, the α-CH bond is 13.6 kcal mol^{-1} weaker than the γ-CH bond and was expected to be the primary site of the free radical oxidation.

The conclusion about the concerted mechanism of the dioxirane oxidation of CH bonds does not exclude, however, *partial diradical character* of the transition state of the reaction (Chart 1a). In addition, dioxiranes can encompass both electron-accepting and electron-donating properties.[7] The electrophilic properties of dioxiranes are due to the low-lying antibonding σ*-like orbital of the O−O bond, and the donating (nucleophilic) properties may ensue from the π*-like out-of-phase combination of the nonbonding orbitals of the oxygen atoms (Chart 1d). Therefore, electron charge-transfer either from the substrate to the dioxirane (Chart 1b) or in the reverse direction (Chart 1c) can take place in the concerted transition state.

The regioselectivity of the dioxirane oxidation will depend on whether there is a preferred character of the

Chart 1

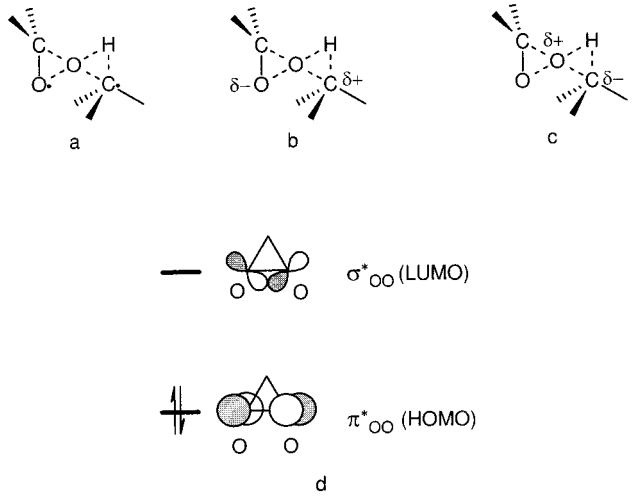

Scheme 3

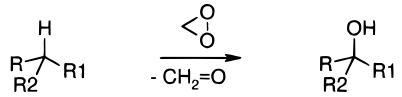

1a R = R1 = R2 = H; **1b** R = R1 = H, R2 = Me; **1c** R = H, R1 = R2 = Me;

1d R = R1 = R2 = Me

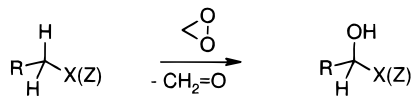

2a R = H, X = NH_2; **2b** R = H, X = OH; **2c** R = Me, X = OH;

2d R = H, Z = CHO

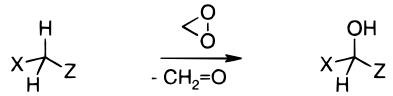

3a X = OH, Z = CHO; **3b** X = NHCHO, Z = $CONH_2$

transition state shown in Chart 1a−c and on the extent to which substituents at the reaction center of the substrate will promote or oppose this character. Experimentally observed regioselectivities[2,3] are consistent with the development of partial radical or carbocationic character at the C atom of the CH bond being oxidized, but not carbanionic character. The problem of establishing the preferred character of the concerted transition state can, in principle, be solved theoretically using high-level ab initio computations.

In the present work, the oxidation of the CH bonds in homo- (**1a**−**d**) and heterosubstituted alkanes (**2a**−**d** and **3a,b**) by the parent dioxirane (Scheme 3) has been studied theoretically. Properties of the latter should be similar to the properties of DMD, which is widely used in experimental works.[1−5]

Substrates were chosen on the basis of the following considerations. First, various levels of theory can be tested for the parent system, methane−dioxirane. Second, analysis of the transition state character can be

(6) Yu, D.; Rauk, A.; Shustov, G. V.; Block, D. A.; Armstrong, D. A., to be published. Results communicated at the Fifth North American Chemistry Meeting, Cancun, Mexico, Nov 11−15, 1997.

(7) (a) Cantos, M.; Merchan, M.; Tomás-Vert, F.; Roos, B. O. *Chem. Phys. Lett.* **1994**, *229*, 181. (b) McDouall, J. J. W. *J. Org. Chem.* **1992**, *57*, 2861. (c) Bach, R. D.; Andrés, J. L.; Owensby, A. L.; Schlegel, H. B.; McDouall, J. J. W. *J. Am. Chem. Soc.* **1992**, *114*, 7207. (d) Houk, K. N.; Liu, J.; DeMello, N. C.; Condorski, K. R. *J. Am. Chem. Soc.* **1997**, *119*, 10147. (e) Miaskiewicz, K.; Teich, N. A.; Smith, D. A. *J. Org. Chem.* **1997**, *62*, 6493. (f) Jenson, C.; Liu, J.; Houk, K. N.; Jorgensen, W. L. *J. Am. Chem. Soc.* **1997**, *119*, 12982.

made more easily from comparison of relative energies, geometries, and charge distributions of the transition states for substrates **2a**−**d** and **3a,b**, which contain strong electron donors (NH_2, OH) and/or acceptors (carbonyl). Third, the reactions of oxidation of isobutane (**1d**) and *N*-formylglycine amide (**3b**) model the probable γ- and α-directions of the dioxirane oxidation of leucine derivatives.[8]

In general, the regioselectivity of the dioxirane oxidation is an important point for comparison of theoretical predictions made here and the experimental data.[1−5] The reactions of the homosubstituted substrates **1a**−**d** model the selective dioxirane oxidations of primary, secondary, and tertiary CH bonds in hydrocarbons;[1,3a,4c] the oxidations of ethanol (**2c**) and glycolaldehyde (**3a**) are a model of the selective oxidation of 1,2-diols[10a,b] and their isopropylidene derivatives[10b,c] into α-hydroxy ketones.

A theoretical model for the concerted oxygen insertion into hydrocarbons was described previously[11] using water oxide (H_2O−O) as the oxidizing agent. We expect the properties of dioxiranes to be quite different from that of water oxide.

During the course of the present work, we became aware of an independent study on the same subject.[12] Houk and Du investigated the CH oxidation of methane with the parent dioxirane and oxidation of methane, ethane, propane, and isobutane with 3-cyanodioxirane theoretically using similar methodology to ours. Their conclusion about a partial diradical character and polarization of the concerted transition state is in accord with ours.

Computational Methods

All ab initio calculations presented here were performed with the Gaussian 94 system of programs.[13] The geometry optimizations and frequency calculations were carried out at the B3LYP hybrid density functional theory level with the internal 6-31G* and 6-311+G** basis sets and also at the second-order Møller−Plesset (MP2) theoretical level using the smaller basis set (except for the parent system), using procedures implemented in the Gaussian molecular orbital package. Harmonic frequency analysis verified the nature of the stationary points as minima (all real frequencies) or as transition structures (one imaginary frequency) and was used to provide an estimate of the zero-point vibrational energies (ZPVE). Zero-point corrections (ΔZPVE) were scaled by a 0.98 factor for the B3LYP level and by 0.967 for the MP2 level.[14] Activation energies for the oxidation of methane were also obtained by MP4(SDTQ) and QCISD(T) single-point calculations using the 6-31G* and 6-311+G** basis sets. In the cases of the MP2, MP4(SDTQ), and QCISD(T) calculations, the frozen core approximation was used. Total energies and ZPVEs of the parent dioxirane, substrates **1a**−**d**, **2a**−**d**, **3a,b**, and the corresponding transition structures are given in Tables S-1 and S-2 of the Supporting Information.

The intrinsic reaction coordinate (IRC)[15] path was traced in order to check the B3LYP/6-31G* and MP2/6-31G* energy profiles for the reaction of methane with the parent dioxirane. Analysis of the electronic properties of the B3LYP and MP2 transition structures for this reaction was performed via natural bond orbital (NBO) analysis.[16] The search for a transition state connecting the reactants (methane + dioxirane) with the radical pair (methyl radical + hydroxymethoxyl radical) was carried out using the synchronous transit-guided quasi-Newton method of transition state optimization (QST2).[17] A methane-dioxirane complex with a H_3CH- - -O intermolecular distance of 2.264 Å (the first point of the IRC) and a complex of the separately optimized methyl radical and hydroxymethoxyl radical with a H_3C- - -HO intermolecular distance of 3.5 Å were used for the QST2-B3LYP/6-31G* calculation as the initial reactants and final products, respectively.

The IRC-B3LYP/6-31G* calculations were performed also for the oxidations of isobutane (**1d**) and *N*-formylglycine amide (**3b**).

The effects of dielectric medium were simulated by single-point SCRF calculations with the IPCM model[18] as implemented in Gaussian 94. Heat capacities and entropy corrections were made using scaled (0.98) B3LYP/6-311+G** frequencies and standard statistical procedures within the rigid rotator−harmonic oscillator model[19] to determine enthalpies and free energies for the oxidation of isobutane at 298 K.

It should be noted that both the B3LYP and MP2 methods have been successfully used for computing dioxirane oxidations of sulfides,[7b] sulfoxides,[7b] alkenes,[7c,d,f] and amines.[7e] We will show here that the MP2 method is *not* appropriate for the description of the dioxirane oxidation of the CH bonds.

Results and Discussion

The Parent System: Methane + Dioxirane. Because B3LYP and MP2 procedures yield very different pictures for the mechanism of O insertion into the CH bond, we describe them separately.

The B3LYP Picture. B3LYP/6-31G* and B3LYP/6-311+G** transition structures are given in Table 1 and shown in Figure 1. The two basis sets give very similar geometric results. The discussion below refers primarily to the larger basis set. In the transition structure, the O1−O2 bond is substantially broken, the bond from the migrating hydrogen (H1) to C2 (1.42 Å) is quite elongated, and its distance to O1 (1.09 Å) is only 0.1 Å longer than a normal OH bond. The C1−O2 bond, which becomes the double bond of formaldehyde, has shortened significantly and the C1−O1 bond, which is eventually lost, has stretched appreciably. The C2H1O1 angle, 123°, is far from linearity. This suggests concurrent formation of the C2−O1 bond, although the C2−O1 distance (2.19 Å) is still very long. The migrating hydrogen, H1, is not far out of the plane of the dioxirane, 31°, indicating involvement of the O−O antibonding orbital of the

(8) *N*-Formylalanine amide would be a better model for the reactivity of the α-CH bond of leucine. We note, however, that the bond dissociation energy of the α-CH bond of **3b** is only 1 kcal mol^{-1} higher than of the corresponding alanine[9] and leucine[6] derivatives.

(9) Rauk, A.; Yu, D.; Armstrong, D. A. *J. Am. Chem. Soc.* **1997**, *119*, 208.

(10) (a) D'Accolti, L.; Detomaso, A.; Fusco, C.; Rosa, A.; Curci, R. *J. Org. Chem.* **1993**, *58*, 3600. (b) Bovicelli, P.; Lupattelli, P.; Sanetti, A. *Tetrahedron Lett.* **1995**, *36*, 3031. (c) Curci, R.; D'Accolti, L.; Dinoi, A.; Fusco, C.; Rosa, A. *Tetrahedron Lett.* **1996**, *37*, 115.

(11) Bach, R. D.; Andrés, J. L.; Su, M.-D.; McDouall, J. J. W. *J. Am. Chem. Soc.* **1993**, *115*, 5768.

(12) Houk, K. N.; Du, X. *J. Org. Chem.*, 1998, submitted.

(13) Frisch, M. J.; Trucks, G. W.; Schlegel, H. B.; Gill, P. M. W.; Johnson, B. G.; Robb, M. A.; Cheeseman, J. R.; Keith, T.; Petersson, G. A.; Montgomery, J. A.; Raghavachary, K.; Al-Laham, M. A.; Zakrzewski, V. G.; Ortiz, J. V.; Foresman, J. B.; Cioslowski, J.; Stefanov, B. B.; Nanayakkara, A.; Challacombe, M.; Peng, C. Y.; Ayala, P. Y.; Chen, W.; Wong, M. W.; Andres, J. L.; Replogle, E. S.; Gomperts, R.; Martin, R. L.; Fox, D. J.; Binkley, J. S.; Defrees, D. J.; Baker, J.; Stewart, J. P.; Head-Gordon, M.; Gonzalez, C.; Pople, J. A. *Gaussian 94, Revisions D.2 and E.2*, Gaussian, Inc., Pittsburgh, PA, 1995.

(14) Scott, A. P.; Radom, L. *J. Phys. Chem.* **1996**, *100*, 16502.

(15) (a) Gonzalez, C.; Schlegel, H. B. *J. Phys. Chem.* **1990**, *94*, 5523. (b) Gonzalez, C.; Schlegel, H. B. *J. Phys. Chem.* **1991**, *95*, 5853.

(16) Glendening, E. D.; Reed, A. E.; Carpenter, J. E.; Weinhold, F. NBO Version 3.1.

(17) Peng, C.; Schlegel, H. B. *Isr. J. Chem.* **1993**, *33*, 449.

(18) Foresman, J. B.; Keith, T. A.; Wiberg, K. B.; Snoonian, J.; Frisch, M. J. *J. Phys. Chem.* **1996**, *100*, 16098.

(19) McQuarrie, D. A. *Statistical Thermodynamics*; Harper & Row: New York, 1973.

Table 1. Potential Energy Barriers[a] (kcal mol^{-1}) for Oxidation of Methane with the Parent Dioxirane

level	E_{rel}
B3LYP/6-31G*	39.8
MP4(SDTQ)/6-31G*//B3LYP/6-31G*	40.8
QCISD(T)/6-31G*//B3LYP/6-31G*	42.9
B3LYP/6-311+G**	32.9
MP4(SDTQ)/6-311+G**//B3LYP/6-311+G**	28.5
QCISD(T)/6-311+G**//B3LYP/6-311+G**	32.6
MP2/6-31G*	40.8
MP4(SDTQ)/6-31G*//MP2/6-31G*	25.3
QCISD(T)/6-31G*//MP2/6-31G*	37.1
MP2/6-311+G**	31.7
MP4(SDTQ)/6-311+G**//MP2/6-311+G**	15.2
QCISD(T)/6-311+G**//MP2/6-311+G**	29.5

[a] Relative to the reactants, including $\Delta ZPVE$.

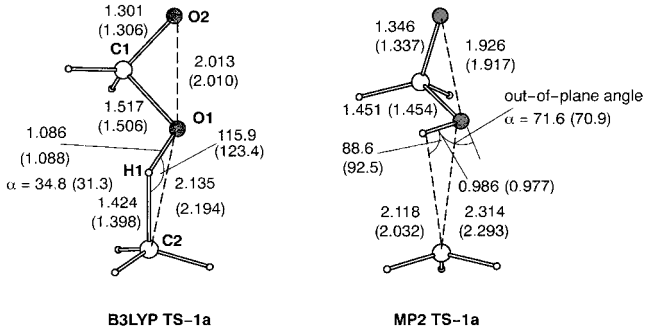

Figure 1. B3LYP and MP2 structures of the concerted transition state for the oxidation of methane with the parent dioxirane calculated with the 6-31G* and 6-311+G** (in parentheses) basis sets. Bond lengths are given in angstroms and angles in degrees.

dioxirane in determining the geometry of the TS. The primarily electrophilic character of the dioxirane is reinforced by NBO population analysis, which indicates a modest transfer of 0.124e from methane to dioxirane (net charge on the CH_3 group is +0.124e). A large dipole moment, 5.7 D, is also predicted for **TS-1a**, more than twice as large as for dioxirane itself (2.8 D). IRC calculations with the smaller basis set verify that **TS-1a** lies on the pathway for the conversion of methane and dioxirane to methanol and formaldehyde with no other stationary points between the reactants and products (Figure 2).

The course of the reaction as displayed in the sequence of structures shown in Figure 2 excludes the possibility that product evolution proceeds by rearrangement to, and decomposition of, an intermediate hemiketal, as suggested by Minisci and co-workers.[5a−c] However, it is clear from inspection of the geometry achieved after the transition structure that the O1−H1 bond is fully formed while the C2−O1 bond of the product is exceedingly long (Figure 2). This suggests the possibility of a *division* of the reaction path *subsequent* to the transition state. One channel, shown in Figure 2, leads directly to the products (formaldehyde and methanol) and corresponds to the concerted electrophilic oxygen insertion mechanism responsible for the retention of stereochemistry. The other channel would result in the evolution of a (solvent-caged, singlet spin coupled) radical pair for which there is ample evidence.[5] Such a splitting of the intrinsic reaction coordinate occurs at a bifurcation point.[20] The transition state for the recombination of the radical pair (methyl radical + hydroxymethoxyl radical) into methane and dioxirane was located by a QST2-B3LYP/6-31G* calculation and proved to be identical to **TS-1a**. This is supporting evidence that there is a bifurcation point on the potential energy surface that occurs *after* the **TS-1a**. By recalculation of the Hessian at successive points along the IRC, it was possible to locate the actual bifurcation point for the parent system 2.0 kcal mol^{-1} below **TS-1a**. This is shown by the solid black dot in Figure 2 at the head of the dashed line leading to the radical pair. Unfortunately, it is not possible at this time to estimate the branching ratio of the two paths.

An activation barrier of 31 ± 2 kcal mol^{-1} is obtained with the larger basis set and supported by MP4 and QCISD(T) calculations. The smaller 6-31G* basis set leads to an overestimation of the barrier by about 10 kcal mol^{-1}.

The MP2 Picture. Transition structures obtained at MP2/6-31G* and MP2/6-311+G** levels are given in Table 1 and Figure 1. Again, the two basis sets give very similar geometric results, and the discussion below refers primarily to the larger. In the transition structure, the O1−O2 bond (1.92 Å) is substantially broken, and the migrating hydrogen (H1) has essentially left C2 (C2−H1 = 2.03 Å) and formed a bond to O1 (H1−O1 = 0.98 Å). The C1−O2 bond (1.34 Å), which becomes the double bond of formaldehyde, has not shortened as much as in the B3LYP picture nor has the stretching of the C1−O1 bond (1.45 Å) progressed as far. The C2H1O1 angle, 92°, is much farther from linearity, and H1 is 71° out of the plane of the dioxirane. The mechanistic picture provided by MP2 is that of prior proton abstraction in preparation for the involvement of the O−O antibonding orbital of the (now protonated) dioxirane in the formation of the C2−O1 bond, which, however, is not as developed as in the B3LYP picture. The primarily nucleophilic character of the dioxirane is apparent from NBO population analysis, which indicates a significant carbanionic character of the methyl carbon (net charge on the CH_3 group is −0.218e). A much smaller dipole moment, 2.05 D, is predicted for **TS-1a**, somewhat smaller than for dioxirane itself (2.7 D). The IRC calculations (with the smaller basis set) were limited to a shorter reaction path segment due to convergence problems.

The activation barrier of 30 ± 1 kcal mol^{-1} obtained with the larger basis set is virtually the same as the B3LYP value. It is supported by the QCISD(T) calculations but not by MP4, which reduce the barrier by half (Table 1). With the smaller 6-31G* basis set, MP2 theory predicts a larger barrier in parallel to the B3LYP results, and this larger value again is supported at the QCISD(T) level but not MP4.

In summary, the B3LYP and MP2 theoretical methods yield divergent pictures of the transition structures and by extension, of the mechanistic details of the reaction. The B3LYP picture suggests electrophilic attack by the dioxirane onto the substrate CH bond, initiating hydride-like transfer of the H atom and the development of carbocationic character in the remainder of the substrate. If this picture is maintained for substrates other than methane, then the implications for the effects of substituents in the substrate is transparent: substituents that

(20) A bifurcation point occurs when one (or more) of the vibrational modes orthogonal to the reaction coordinate achieves a zero force constant; i.e., a path down a valley becomes a ridge dividing two valleys. IRC calculations frequently "crash" at bifurcation points, which are common, especially if there is a reduction of symmetry along the path. The present IRC calculations do not "crash".

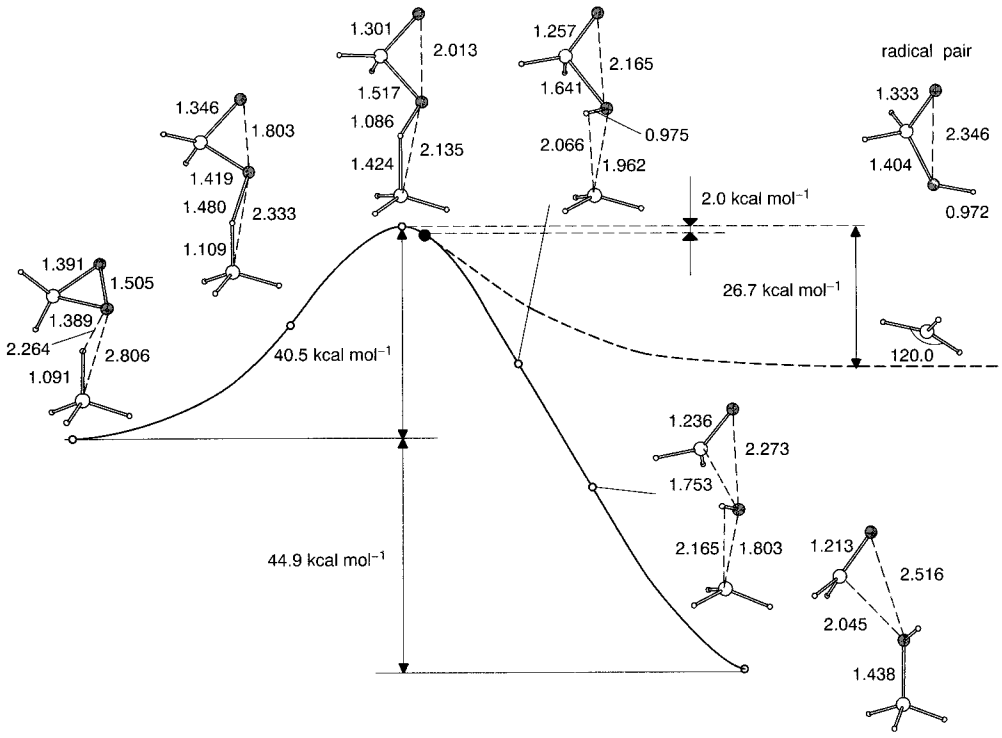

Figure 2. Schematic representation of the concerted (solid line, derived with the IRC-B3LYP/6-31G* calculation) and free radical (dashed line) reaction pathways for the parent methane−dioxirane system. The solid black dot stands for the bifurcation point. Bond lengths are given in angstroms and angles in degrees.

stabilize the carbocationic center (i.e., electron donors, −X:) will reduce the activation barrier, and substituents that do not (i.e., electron acceptors, −Z) may actually raise the activation barrier and hinder the reaction. The large dipole moment predicted for the TS suggests that the reaction will be favored in more polar solvents and relative to the gas phase. Indeed, experimental results, and the studies on the substituted alkanes we discuss below, are consistent with the B3LYP picture. On the other hand, the MP2 picture suggests initial proton abstraction with the development of substantial carbanionic character in the substrate. If *this* character is intrinsic to the oxidation mechanism, then Z-type substituents such as carbonyl should accelerate the reaction and X-type substituents such as alkyl, amino, or hydroxy may actually hinder the reaction. Overlying these considerations is some diradical character of the TS as predicted by either theoretical approach.

Conformational Stereochemistry of the Transition States. In the cases of unsymmetrical substrates **1b,c**, **2a**−**d**, and **3a,b**, formation of isomeric transition states, which differ by the mutual orientation of the attacking dioxirane and the substituents at C2, is possible as shown in Chart 2. We focus attention here on the B3LYP/6-311+G** results, noting differences due to basis set and theoretical method in passing.

In the oxidation of the alkanes, ethane (**TS-1b**) and propane (**TS-1c**), at all theoretical levels, the dioxirane approaches from the direction of minimum steric interaction with the methyl groups at C2 (Chart 2b), i.e., at least one group is anti-oriented relative to CH_2 of dioxirane. In the transition states for the oxidation of methanol (**TS-2b**) and ethanol (**TS-2c**) (Figure 3), the dioxirane approaches in the gauche position with respect to the hydroxy group of the substrate (Chart 2c,d). Such an orientation is apparently a consequence of the secondary orbital interaction between the nonbonding n orbital of the O1 atom and the antibonding σ^* orbital of the C2−O3 bond, i.e., a kind of the anomeric effect. The carbonyl group of acetaldehyde also adopts a gauche orientation (**TS-2d**), which is again attributable to a secondary orbital interaction between the n orbital of dioxirane and the π^* orbital of the carbonyl group. In this case, an anti structure (anti-**TS-2d**) is also found with the smaller, but not the larger basis set. Similarly, the smaller basis set yields both gauche and anti TSs for the reaction with methylamine, but only the anti structure, anti-**TS-2a**, is a minimum with the larger basis set, reflecting the lower acceptor ability of the C−N antibonding σ^* orbital. Only small basis set MP2 calculations were carried out for these systems, and only anti structures were found in each case.

Probably, the secondary orbital interaction controls also the gauche approach of the dioxirane to the doubly substituted substrates, glycolaldehyde (**TS-3a**) and *N*-formylglycine amide (**TS-3b**) (Chart 2e).

Relationship between the Transition-State Character and the Nature of Substituents in the Substrate. The differences in the character and structure of the B3LYP and MP2 transition states for the oxidation of methane (electrophilic O insertion at B3LYP, proton transfer at MP2) remain in the entire series of the studied substrates **1b**−**d**, **2a**−**d**, and **3a** (Tables 3 and 4, Figures 3−5).

The decrease of the out-of-plane angle α and the increase of the O1H1C2 angle in the B3LYP transition state as the electron-donating ability of the substituent (X:) at C2 is increased, for example, in the series of ethane (X: = CH_3) − methanol (X: = OH) − methylamine (X: = NH_2), indicate that this transition state acquires increasing *hydride-transfer character*. The electrons of the n orbital of the electron-donating X: group (NH_2, OH)

Chart 2

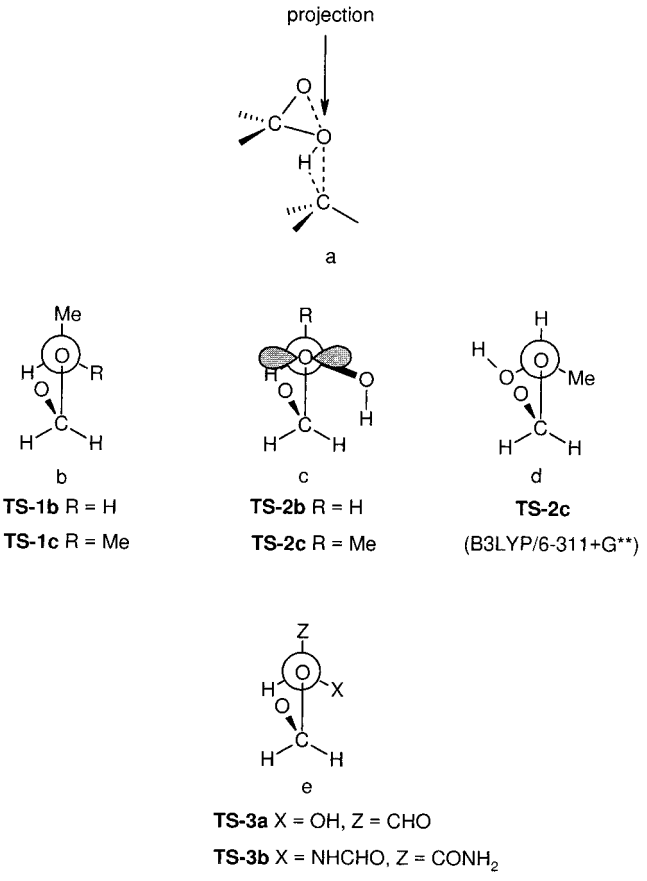

compensate for the electron deficiency arising at the C2 atom (Scheme 4a). As a result, structures **B3LYP TS-2a,b** are characterized by the C2−X: bonds (Figure 3), which are substantially shorter than the corresponding bonds in the initial substrates (1.465 Å for the C−N bond in methylamine, 1.419 Å for the C−O bond in methanol). **B3LYP TS-2a** is a practically pure case of hydride transfer. In this structure (Figure 3), the H1 atom lies in the plane of the dioxirane ring (the out-of-plane angle α is equal to 0°), the O1H1C2 angle is close to 180°, and the C1−N bond is shortened by 0.075 Å in comparison with methylamine. It is interesting to note the almost identical O1−H1 (1.248 Å) and H1−C2 (1.258 Å) distances in that case. As expected, the B3LYP activation energies for the oxidation of substrates **1b**, **2a,b** are decreased (Table 2) with increasing electron-donating ability of the X: substituent.

The presence of an electron-withdrawing carbonyl group at the reaction center of the substrate diminishes the hydride transfer character of the B3LYP transition state and destabilizes it. The B3LYP transition state for the oxidation of the α-CH bond in acetaldehyde (**TS-2d**) is a most pronounced example of this. In **TS-2d** (Figure

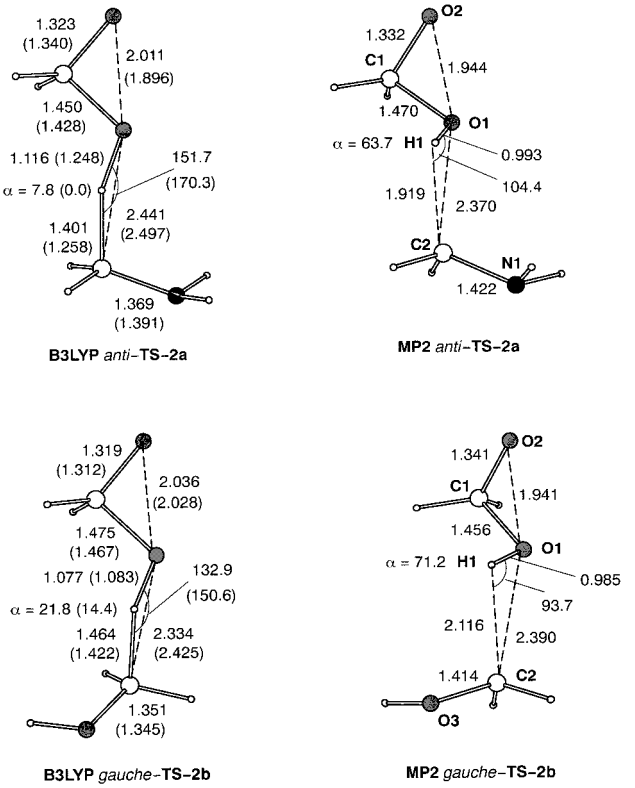

Figure 3. B3LYP and MP2 structures of the concerted transition state for the CH oxidation of methylamine (**2a**) and methanol (**2b**) with the parent dioxirane calculated with the 6-31G* and 6-311+G** (in parentheses) basis sets. Bond lengths are given in angstroms and angles in degrees.

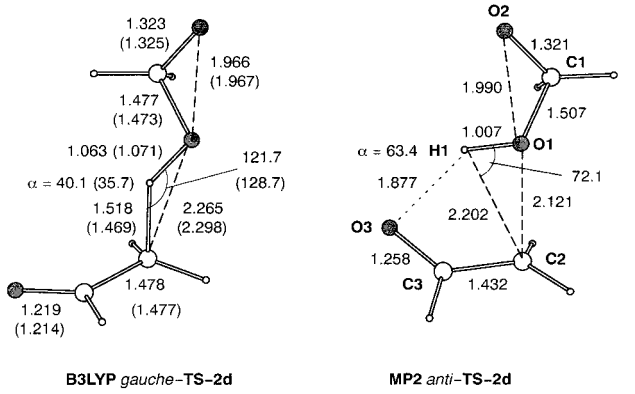

Figure 4. B3LYP and MP2 structures of the concerted transition state for the α-CH oxidation of acetaldehyde (**2d**) with the parent dioxirane calculated with the 6-31G* and 6-311+G** (in parentheses) basis sets. Bond lengths are given in angstroms and angles in degrees.

4), the out-of-plane angle α is greater and the O1H1C2 angle is smaller than the corresponding angles in the transition state for the oxidation of ethane (**TS-1b**) (Table 3). Correspondingly, the potential barriers for the oxidation of acetaldehyde are *higher* by 4.0 kcal mol^{-1} (by 2.1 using 6-31G*) than the barriers for the oxidation of ethane. This result is consistent with the noninterference of the acetone byproduct of DMD oxidations and with the ability to use acetone as a solvent.

Contrary to the B3LYP and experimental experience but consistent with the MP2 picture presented above, an abrupt lowering of the potential barrier is predicted by the MP2 method (Table 2) in the oxidation of the α-CH

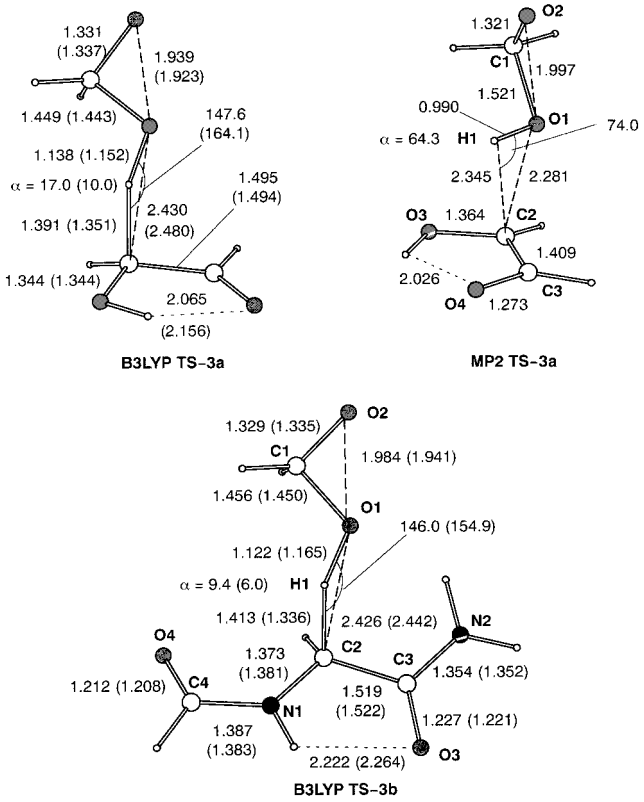

Figure 5. B3LYP and MP2 structures of the concerted transition state for the α-CH oxidation of glycolaldehyde (**3a**) and *N*-formylglycine amide (**3b**) with the parent dioxirane calculated with the 6-31G* and 6-311+G** (in parentheses) basis sets. Bond lengths are given in angstroms and angles in degrees.

bond in acetaldehyde. It is also confirmed by the geometry of **MP2 TS-2d** (Table 4, Figure 4), in which a significant shortening of the C2−C3 bond and an elongation of the C3−O3 bond are observed. Such structural changes are caused by delocalization of an abundant electron density arising on the C2 atom upon transferring the H1 proton (Scheme 4b). Unlike the carbonyl group, the amino group is unable to delocalize effectively the abundant electron density of the C2 atom. Therefore, the activation energy for the oxidation of the CH bond in methylamine predicted at the MP2/6-31G* level is 12.1 kcal mol^{-1} greater than the energy predicted at the B3LYP/6-31G* level. For the oxidation of ethane, this difference is just 4.1 kcal mol^{-1}. Nevertheless, examination of the MP2 geometries of the transition states for the oxidation of the substrates with the n-donating substituents (X:) at C2−methanol and methylamine allows us to assume the existence of a stabilizing interaction between the group X: and reaction center C2. Indeed, the C2−N1 and C2−O3 bonds in the substrate fragment of **MP2 TS-2a,b** (Figure 3) are somewhat shorter than the corresponding bonds in substrates **2a,b** (1.465 Å for the CN bond in methylamine and 1.424 Å for the CO bond in methanol). Besides, the conformations around the C2−N1 and C2−O3 bonds (Figure 3) indicate the maximum overlap of the n orbital of the heteroatom with the breaking C1−H1 bond and/or forming C2−O1 bond. Apparently, it is caused by a partial diradical character of the MP2 transition states, at which the three-electron interaction (Scheme 4c) is realized. The lowering of the MP2 potential barriers of the oxidation

Scheme 4

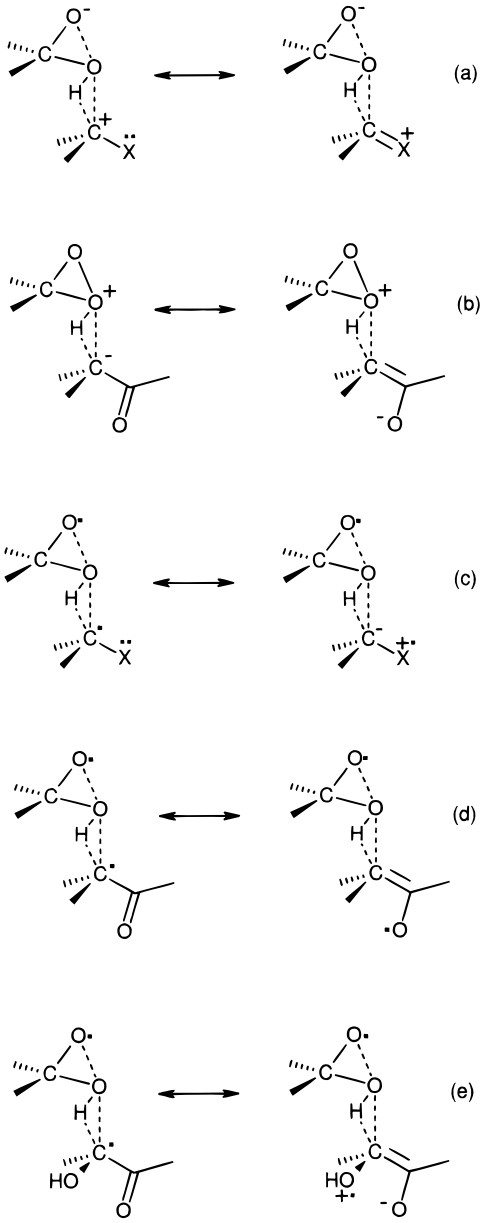

with increasing electron-donating ability of the substituent X: in the series of ethane − methanol − methylamine and with accumulating methyl groups at C2 in the series of methane − ethane − propane − isobutane (Tables 1 and 2) also reflects the partial diradical character of the MP2 transition states. In the case of **MP2 TS-2d**, the partially singly occupied orbital of the reaction center can interact with the antibonding π^* orbital of the carbonyl group (Scheme 4d).

To the extent that radical character at the reaction center of the substrate is important, the most favorable situation for delocalization of the unpaired electron occurs when both n donor and π acceptor groups are present, the nonadditive effect of the two groups being referred to as captodative stabilization[21a] (mero-stabilization[21b]).

The two systems, **TS-3a,b**, in which captodative stabilization of radical character can occur, are predicted to

(21) (a) Viehe, H. G.; Janousek, Z.; Merenyi, R. *Acc. Chem. Res.* **1985**, *18*, 148. (b) Balddock, R. W.; Hudson, P.; Katritzky, A. R.; Soti, F. *J. Chem. Soc., Perkin Trans. 1* **1974**, 1422. For a review see: (c) Sustmann, R.; Korth, H.-G. *Adv. Phys. Org. Chem.* **1990**, *26*, 131.

Table 2. Potential Energy Barriers[a] (kcal mol^{-1}) for Oxidation of Substrates 1b−d, 2a−d, and 3a,b with the Parent Dioxirane

substrate	TS	B3LYP/6-31G*	B3LYP/6-311+G**	MP2/6-31G*
ethane	**TS-1b**	33.4	25.9	37.5
propane	**TS-1c**	28.5	20.5	35.2
isobutane	**TS-1d**	24.3	15.7	33.0
methylamine	*anti*-**TS-2a**	16.6	10.4	28.7
	gauche-**TS-2a**	16.6		
methanol	**TS-2b**	26.0	19.9	29.9
ethanol	**TS-2c**	21.0	14.4	27.7
acetaldehyde	*anti*-**TS-2d**	35.6		19.9
	gauche-**TS-2d**	35.5	29.9	
glycolaldehyde	**TS-3a**	20.4	16.2	7.4
N-formylglycine amide	**TS-3b**	18.9	15.0	

[a] Relative to the reactants, including $\Delta ZPVE$.

Table 3. Selected Calculated Geometrical Parameters[a] of the TS for the Oxidation of Hydrocarbons 1b−d with the Parent Dioxirane

	O1- - -H1	O1- - -C2	C2- - -H1	O- - -O	C1−O1	C1−O2	C2−C[b]	O1H1C2	α[c]
				TS-1b					
B3LYP/6-31G*	1.081	2.208	1.433	2.026	1.503	1.304	1.496	122.2	30.3
B3LYP/6-311+G**	1.083	2.286	1.407	2.024	1.491	1.311	1.492	132.8	25.1
MP2/6-31G*	0.988	2.321	2.039	2.321	1.455	1.343	1.501	93.6	69.7
				TS-1c					
B3LYP/6-31G*	1.069	2.289	1.457	2.044	1.492	1.307	1.499	129.3	26.4
B3LYP/6-311+G**	1.070	2.385	1.431	2.047	1.482	1.314	1.493	144.5	18.3
MP2/6-31G*	0.989	2.322	2.000	2.322	1.462	1.340	1.503	96.0	68.5
				TS-1d					
B3LYP/6-31G*	1.061	2.373	1.479	2.063	1.487	1.309	1.503	137.7	19.7
B3LYP/6-311+G**	1.092	2.464	1.397	2.025	1.464	1.322	1.503	163.8	0.2
MP2/6-31G*	0.992	2.314	2.314	1.874	1.468	1.337	1.507	98.7	66.7

[a] Bond lengths in angstroms, angles in degrees; numbering of atoms as in Figure 1. [b] The C−C bond trans-oriented with respect to the dioxirane ring. [c] The out-of-plane angle between the O1−H1 bond and the dioxirane ring plane.

Table 4. Selected Calculated Geometrical Parameters[a] of the TS for the Oxidation of Functionally Substituted Substrates 2a−d with the Parent Dioxirane

	O1- - -H1	O1- - -C2	C2- - -H1	O- - -O	C1−O1	C1−O2	C2−C/Z	O1H1C2	α[b]
				gauche-**TS-2a**					
B3LYP/6-31G*	1.116	2.446	1.390	2.014	1.452	1.321	1.373 (C2N1)	154.8	10.7
				TS-2c					
B3LYP/6-31G*	1.091	2.402	1.435	2.028	1.464	1.316	1.357 (C2O3) 1.495 (C2C3)	143.6	13.9
B3LYP/6-311+G**	1.162(	2.456	1.317	1.953	1.449	1.330	1.362 (C2O3) 1.499 (C2C3)	164.3	0.6
MP2/6-31G*	1.000	2.311	1.997	1.923	1.462	1.337	1.448 (C2O3) 1.492 (C2C3)	95.0	70.4
				anti-**TS-2d**					
B3LYP/6-31G*	1.074	2.266	1.484	1.963	1.478	1.320	1.478 (C2C3)	123.9	37.9

[a] Bond lengths in angstroms, angles in degrees; numbering of atoms as in Figure 3. [b] The out-of-plane angle between the O1−H1 bond and the dioxirane ring plane.

have lower activation energies in all cases except **TS-2a** and **TS-2c** (Table 2). Results at the B3LYP/6-31G* level are similar, although the overall changes in the activation barriers at this level are larger. One could conclude that this character is exaggerated with the use of the smaller 6-31G* basis set.

Selectivity. To the extent that both methods incorporate diradical character into the TS, they predict, in accord with experiment,[1,3a] decreasing activation energy for the dioxirane oxidation of alkanes with increasing number of alkyl substituents at the reaction center of the substrate. However, the inadequacy of the MP2 picture of the transition state becomes obvious upon consideration of the selectivity of the oxidation of substrates **2a−d** and **3a**, containing X:- and/or Z-type functional groups. First, the MP2 method predicts a substantially greater stabilizing effect on the transition state for the carbonyl group than for methyl groups and the hydroxy group. If correct, it would mean that DMD and TFMD must oxidize acetone and 1,1,1-trifluoroacetone, respectively, much faster than secondary and tertiary alkanes and alcohols. In fact, acetone solutions of DMD and trifluoroacetone solutions of TFMD[1] are used for the oxidation of the alkanes[3a,c,d,4,5a,b,d] and alcohols.[3b] Second, the considerably lesser relative energy (7.4 kcal mol^{-1}) of the MP2 transition state for the oxidation of glycolaldehyde in comparison with the MP2 transition-state energy (27.7 kcal mol^{-1}) for the oxidation of ethanol means that the oxidation of 1,2-diols must lead to α-diketones and does not come to a stop at the intermediate α-hydroxy ketone stage. In contrast with this prediction, it has been experimentally shown that the dioxirane oxidations of 1,2-diols[10a,b] and their isopropylidene derivatives [10b,c] provide high yields of the α-hydroxy ketones even at an excess of the dioxirane (DMD or TFMD) with respect to the substrate.

Unlike the MP2 picture, the B3LYP picture of the transition state for the dioxirane oxidation is in accord with the experimental findings. Indeed, the B3LYP method predicts a higher potential barrier for oxidation of the α-CH bond in acetaldehyde (model for the oxidation of acetone by DMD) in comparison with the barriers for the oxidation of propane, isobutane (models for the oxidation of secondary and tertiary alkanes), methanol, and ethanol (models for the oxidation of alcohols) (Table 2). Further, the relative energy of the transition state for the oxidation of ethanol (**TS-2c**) is 1.8 kcal mol^{-1} lower than the energy of the transition state of glycolaldehyde (**TS-3a**), in excellent agreement with the experimental observations on the selective dioxirane oxidations of 1,2-diols[10a,b] and their isopropylidene derivatives.[10b,c]

Model for the Oxidation of Peptides and the Influence of Solvent on Selectivity. As mentioned above, the probable γ- and α-directions of the dioxirane oxidation of the leucine derivatives (Scheme 2) can be modeled by the oxidations of isobutane (**1d**) and *N*-formylglycine amide (**3b**), respectively (Scheme 3). According to the IRC-B3LYP/6-31G* calculations, both reactions prefer the concerted pathway directly to the oxidation products. Experimentally, only the tertiary CH bond at the γ-position of leucine is oxidized (Scheme 2).[2] In disagreement with this result, the gas-phase B3LYP/6-311+G** calculations predict a slightly *higher* activation barrier for the oxidation of isobutane than for the oxidation of *N*-formylglycine amide (Table 2). However, the real oxidation of the substituted leucines was carried out in a polar medium, i.e., in CH_2Cl_2. As discussed above, the B3LYP transition states are highly polar and characterized by modest electron charge transfer from the substrate fragment to the dioxirane one. The charge separation in these structures will be increased in a polar medium. In such a case, **TS-1c** will be stabilized to a greater extent than **TS-3b** because the carbonyl group in the latter will oppose an additional electron charge transfer from the substrate to the dioxirane. Indeed, the SCRF calculations using the IPCM model of the polar medium (CH_2Cl_2, $\epsilon = 9.08$) give a decrease of the potential barrier for the oxidation of isobutane by 12.2 kcal mol^{-1} and for the oxidation of *N*-formylglycine amide by only 0.4 kcal mol^{-1}. Thus, in CH_2Cl_2, the activation energy of the oxidation of isobutane is 11.2 kcal mol^{-1} *smaller* than the activation energy of the oxidation of *N*-formylglycine amide, in accord with the experimental γ-selectivity of the dioxirane oxidation of the leucine derivatives in this solvent.[2]

A similar influence of the polar medium on the relative energies of the B3LYP transition states is observed for the ethanol−glycolaldehyde pair (Table 5). The potential barrier for the oxidation of ethanol is lowered by 8.0 kcal mol^{-1} (8.9 with 6-31G*) to 6.4 kcal mol^{-1}, whereas for the oxidation of glycolaldehyde, it is lowered by only 2.4 kcal mol^{-1} (2.9 with 6-31G*) to 13.8 kcal mol^{-1}.

True to form, the polar solvent influences the MP2 potential barriers for the oxidation of ethanol and glycolaldehyde in the opposite direction (Table 5): the relative energy of **MP2 TS-2c** is increased by 4.6 kcal mol^{-1} and of **MP2 TS-3a** is decreased by 2.9 kcal mol^{-1}, in greater disagreement with experiments.[11]

The extraordinarily low barrier, 3.5 kcal mol^{-1}, predicted for the oxidation of isobutane in CH_2Cl_2, corresponds to the enthalpy of activation at 0 K. After corrections for temperature and assuming negligible differential free energy of solution for the gas phase to CH_2Cl_2 transition, the IPCM-B3LYP/6-311+G** calculations give a reasonable value of the free energy of activation for the oxidation of isobutane with the parent dioxirane, $\Delta G^{\ddagger}_{298} = 9.8$ kcal mol^{-1} ($\Delta H^{\ddagger}_{298} = 3.8$ kcal mol^{-1}, $\Delta S^{\ddagger}_{298} = -20.1$ cal mol^{-1} K^{-1}), in CH_2Cl_2. This calculated value of $\Delta G^{\ddagger}_{298}$ is comparable with experimental values for the oxidation of 1,2-*cis*-dimethylcyclohexane (ca. 21 kcal mol^{-1})[3d] and adamantane (ca. 20 kcal mol^{-1})[4c,d] by DMD, taking into account a greater reaction ability of the parent dioxirane in comparison with DMD.

Table 5. Potential Energy Barriers[a] (kcal mol^{-1}) for Oxidation of Substrates 1c,d, 2c, and 3a,b with the Parent Dioxirane Derived with the IPCM Model of Dielectric Medium (CH_2Cl_2, $\epsilon = 9.08$)

substrate	TS	level	E_{rel}
propane	**TS-1c**	B3LYP/6-31G*	19.5
		B3LYP/6-311+G**	9.7
isobutane	**TS-1d**	B3LYP/6-31G*	13.4
		B3LYP/6-311+G**	3.5
ethanol	**TS-2c**	B3LYP/6-31G*	12.1
		B3LYP/6-311+G**	6.4
		MP2/6-31G*	32.3
glycolaldehyde	**TS-3a**	B3LYP/6-31G*	17.5
		B3LYP/6-311+G**	13.8
		MP2/6-31G*	4.5
N-formylglycine amide	**TS-3b**	B3LYP/6-31G*	17.9
		B3LYP/6-311+G**	14.6

[a] Relative to the reactants, including ΔZPVE.

Conclusions

The present results suggest a new mechanism of the dioxirane oxidation of aliphatic CH bonds, which reconciles the apparently contradictory experimental data. A bimolecular electrophilic interaction occurs between the C−H bond and the dioxirane, leading to a highly polar transition state with substantial carbocationic character at the carbon atom of the substrate. At this transition state, the C−H bond is partially broken, the O−H bond is essentially completely formed, and the O−O bond of the dioxirane is substantially broken. Subsequently, the reaction path divides into two channels. One channel corresponds to concerted transfer of the OH group to the carbon atom from which the hydrogen was lost in a concerted manner. Retention of stereochemistry is predicted. Even those systems possessing weak C−H bonds (isobutane, *N*-formylglycine amide) have this channel available to them. The other channel corresponds to separation into an α-hydroxyalkoxyl radical and an alkyl radical, which may then escape the surrounding solvent cage and lead to the host of free-radical-derived reaction products. The common transition state for the two channels then provides a mechanism for "molecule-induced homolysis" of the dioxirane—rupture of the C−H bond occurs simultaneously and is not the result of the hydrogen atom abstraction by a preformed oxy radical. It is important to stress that the proportion of products from electrophilic attack compared to radical derived products will depend primarily on the branching ratio at the bifurcation point and less on whether the reactive species remain trapped in a solvent cage or can escape from it.

All substituent and solvent effects for the dioxirane oxidation of aliphatic CH bonds are satisfactorily reproduced at the B3LYP hybrid density functional theoretical level with the 6-311+G** basis set. Further specific conclusions ensue from the B3LYP picture.

The selectivity of the dioxirane oxidation of the CH bonds in hydrocarbons, alcohols, and 1,2-diols is very satisfactorily reproduced. Agreement between the theoretical predictions and experimental data is improved by taking into account the influence of a dielectric medium. Under these conditions, the γ-regioselectivity of the dioxirane oxidation of leucine derivatives[2] is theoretically reproduced.

The calculated activation parameters ($\Delta G^{\ddagger}_{298} = 9.8$ kcal mol^{-1}, $\Delta H^{\ddagger}_{298} = 3.8$ kcal mol^{-1}, $\Delta S^{\ddagger}_{298} = -20.1$ cal mol^{-1} K^{-1}) of the oxidation of isobutane by the parent dioxirane in CH_2Cl_2 are in reasonable agreement with experimental kinetic data on the dimethyldioxirane oxidation of tertiary alkanes.[3c,d,4c,d]

The electron charge transfer from the substrate to the dioxirane is a key element of the concerted transition state. Electron-donating substituents at the reaction center of the substrate, which are able to compensate an electron deficiency arising at this center, decrease the activation barrier for the dioxirane oxidation. Correspondingly, the presence of electron-withdrawing substituents in the substrate increases the barrier. Hence, side groups of protected amino acids and proteins are more probable points of the dioxirane attack than the α-carbon centers containing the electron-withdrawing carbonyl group, even though the bond dissociation energy of an α-C−H bond is more than 10 kcal mol^{-1} less than a tertiary aliphatic C−H bond.

A solvent of higher polarity promotes the charge separation in the concerted transition state and increases the probability of dioxirane attack on electron-rich sites of the substrate.

The MP2 method is shown to be unsatisfactory. It overestimates the nucleophilic/basic properties of the dioxirane. The MP2 transition state has the character of proton transfer from the substrate to the dioxirane arising from a dominant participation of HOMO (π^*_{OO}) of the dioxirane.

Acknowledgment. The financial support of the Natural Sciences and Engineering Research Council of Canada is gratefully acknowledged.

Supporting Information Available: Tables S-1 and S-2 showing total energies and zero-point vibrational energies of the parent dioxirane, substrates **1a**−**d**, **2a**−**d**, and **3a,b**, and the corresponding transition structures (2 pages). This material is contained in libraries on microfiche, immediately follows this article in the microfilm version of the journal, and can be ordered from the ACS; see any current masthead page for ordering information.

JO9802877